Biocompatibility of Polysulfone Hemodialysis Membranes and Its Mechanisms: Involvement of Fibrinogen and Its Integrin Receptors in Activation of Platelets and Neutrophils

*Yoko Koga ⓘ, †Hiroaki Fujieda, *Hiroyuki Meguro, †Yoshiyuki Ueno, †Takao Aoki, †Keishi Miwa, and *Mie Kainoh

*Department of Pharmacology Laboratory, Pharmaceutical Research Laboratories, Toray Industries, Inc., Kamakura, Kanagawa; and †Department of Medical Devices and Materials Research Laboratory, Advanced Material Research Laboratories, Toray Industries, Inc., Otsu, Siga, Japan

Abstract: Activation of blood cells during hemodialysis is considered to be a significant determinant of biocompatibility of the hemodialysis membrane because it may affect patient health adversely through microvascular inflammation and oxidative stress. This study found very different cell activation among various polysulfone (PSf) hemodialysis membranes. For example, CX-U, a conventional PSf membrane, induced marked adhesion of platelets to its surface and increased surface expression of activated CD11b and production of reactive oxygen species (ROS) by neutrophils; while NV-U, a hydrophilic polymer-immobilized PSf membrane, caused little platelet adhesion and slight CD11b expression and ROS production by neutrophils. Analysis of the molecular mechanisms of the above phenomena on CX-U and NV-U indicated that anti-integrin GPIIb/IIIa antibody blocked platelet adhesion, and that the combination of anti-CD11b (integrin α subunit of Mac-1) and anti-integrin $\alpha v \beta 3$ antibodies blocked ROS production by neutrophils. Plasma-derived fibrinogen, a major ligand of GPIIb/IIIa, Mac-1, and $\alpha v \beta 3$ on membranes, was thus analyzed and found to be more adsorbed to CX-U than to NV-U. Moreover, comparison between five PSf membranes showed that the number of adherent platelets and neutrophil ROS production increased with increasing fibrinogen adsorption. These results suggested that fibrinogen, adsorbed on membranes, induced GPIIb/IIIa-mediated platelet activation and Mac-1/$\alpha v \beta 3$-mediated neutrophil activation, depending on the amount of adsorption. In conclusion, the use of biocompatible membranes like NV-U, which show lower adsorption of fibrinogen, is expected to reduce hemodialysis-induced inflammation and oxidative stress by minimizing cell activation. **Key Words:** Hemodialysis membrane—Biocompatibility—Platelet—Neutrophil—Fibrinogen.

Cell activation, induced by the exposure of blood components to "non-self" hemodialysis (HD) membranes, is frequently observed during dialysis in clinical settings and activation of blood cells is considered to be a significant determinant of HD membrane biocompatibility. Studies of platelet activation and plasma concentrations of platelet factor 4 (PF-4) and β-thromboglobulin (β-TG), which are released from α-granules of platelets on acute platelet activation, reported that all are significantly greater in HD patients [1]. In addition, platelet aggregates or platelet-leukocyte complexes were found in the peripheral circulation of patients on HD treatment [1] and this observation indicates that activated platelets tend to stick to themselves or leukocytes. Studies of leukocyte activation in HD patients showed that cell surface expression of CD11b on leukocytes, a marker for the activation-dependent receptor Mac-1, was increased [2,3] and

that the plasma concentrations of pro-inflammatory cytokines like tumor necrosis factor (TNF) α and interleukin (IL) 6, were higher in HD patients than in healthy subjects (4,5). It has also been reported that intracellular levels of reactive oxygen species (ROS) in leukocytes, and parameters of oxidative stress were increased in HD patients (4,6,7).

The clinical consequences of these HD-induced cell activations have not been well elucidated; however, the increase in various inflammatory mediators and cytotoxic materials can induce and maintain a chronic state of inflammation and oxidative stress, which may lead to HD-associated cardiovascular and other complications (8). Specifically, accelerated atherosclerosis and anemia are very common complications in HD patients and their pathogenesis is closely related to HD-induced oxidative stress. In particular, ROS promote conversion of macrophages to foam cells and endothelial dysfunction in atherosclerosis (7,9,10) and the oxidation of lipids, proteins and nucleic acids by ROS exaggerate renal anemia by shortening the life span of red blood cells (11). Because atherosclerosis-related cardiovascular disease (CVD) is a principal cause of morbidity and mortality in HD patients (6,12), and anemia is also a risk factor for CVD, it is extremely important to reduce such risks if we are to improve prognosis in the HD patient.

In recent years, technological advances in membrane design, chemical composition, and sterilization methods have improved biocompatibility of HD membranes. In particular, polysulfone (PSf) membranes are most commonly used in HD therapy, because of their exceptional biofunctional characteristics such as an improved biocompatibility, a sharp cut-off property for molecular weight, and good water permeability. Several different brands of PSf dialyzer are currently available commercially; however, their membranes cannot be considered equivalent due to their different manufacturing methods, for example, differences in the contained amount of a hydrophilic polymer, polyvinylpyrrolidone (PVP), and different sterilization methods, among others (13). Actual activation of blood cells during HD varied among different PSf dialyzers in clinical studies (14–16). These observations imply that different PSf membranes have different effects on blood cells; however, details of these phenomena and their mechanisms have not been clarified yet.

The purpose of this study was to clarify the biocompatibility of PSf membranes and its mechanisms. To this end, we examined effects of five commercially available PSf type membranes including a variant of PSf, polyethersulfone (PES) on activation of platelets and neutrophils in vitro, and analyzed the molecular basis of the interaction between these cells and adsorbed proteins.

MATERIALS AND METHODS

HD membranes

Technical data on the five HD membranes tested are summarized in Table 1. These fiber HD membranes were obtained from commercial dialyzers; APS-SA (Asahi Kasei Medical, Tokyo, Japan), PES-SEαeco (Nipro, Osaka, Japan), Fx-CorDiax (Fresenius Medical Care Japan, Tokyo, Japan), CX-U and NV-U (Toray, Tokyo, Japan), respectively.

We measured the thickness of the swollen surface layer of the polymer as a parameter of the membrane surface structure (Table 1). For measurement of the swollen surface layer, HD membranes were cut lengthwise into half to expose their inner surfaces and then placed on a steel disk. After the membranes were immersed into pure water, they were mounted on the stage of an atomic-force microscope (AFM, Shimadzu, Kyoto,

TABLE 1. *Technical data concerning the hollow-fiber hemodialysis (HD) membranes tested and the thickness of the swollen layer of the inner surface of HD membranes*

Membranes	Materials of membrane	Inner diameter (μm)	Wall thickness (μm)	Sterilization	Thickness of swollen layer (nm)
CX-U	PSf	200	40	Gamma-ray	5.3 ± 0.4
NV-U	PSf	200	40	Gamma-ray	10.4 ± 1.3
APS-SA	PSf	185	45	Gamma-ray	7.9 ± 1.0
PES-SEαeco	PES	200	40	Gamma-ray	5.5 ± 0.7
FX-CorDiax	PSf	185	35	Steam	7.0 ± 1.0

PSf, polysulfone; PES, poly(ethersulfone).
Thickness of swollen layer of HD membranes inner surface was estimated by the force-distance curve measured by atomic-force microscopy. Data of thickness of swollen layer are presented as mean ± SEM of eight independent experiments. There were statistically significant differences between CX-U and NV-U ($P < 0.01$), and between NV-U and PES-Seαeco ($P < 0.01$). (Tukey's multiple comparison).

Japan) and measured immediately in contact mode, using a triangular silicon nitride cantilever (type NP-S, Digital Instruments, Santa Barbara, CA, USA). The force-distance curve was obtained by measuring the probe-sample interaction force along with the vertical displacement of the cantilever during the process of approaching the sample (Supporting Information Figure S1). The probe-sample force was estimated from the deflection of the cantilever according to Hooke's law (17). The length of the curved portion in the force–distance curve was defined as the thickness of the swollen surface layer because the swollen layer on membrane surfaces causes this curvature.

Surface element composition on the inner surface of the HD membranes was measured by X-ray photoelectron spectroscopy (ESCALAB220iXL; Thermo VG Scientific, East Grinstead, UK) equipped with a monochromatized Al Kα source (1486.6 eV) of 0.15 mm diameter operating at a voltage of 10.0 kV, a current of 5 mA, and a photoelectron escape angle of 90°.

Reagents

Anti-GPIa (CD29) antibody (Clone:4B4) was purchased from Beckman Coulter (Brea, CA, USA). Anti-GPIb (CD42b) antibody (Clone: 303908), PE-conjugated anti-activated CD11b antibody (clone: CBRM1/5), PE-conjugated anti-CD11b and antibody (clone: ICRF44), its isotype control, PE-conjugated mouse IgG1 (clone: MOCP-21), and anti-αvβ3 antibody (clone: 23C6), were purchased from BioLegend (San Diego, CA, USA). Anti-CD11b antibody (clone: CBRM1/5) was purchased from eBioscience (San Diego, CA, USA). An isotype control, mouse IgG1 (clone: MPOC-21) for anti-αvβ3 antibody and anti-CD11b antibody was purchased from BioXCell (West Lebanon, NH, USA). Cyclo-GRGDSP (GRGDSP, N to C cyclized, Cyclo-[Gly-Arg-Gly-Asp-Ser-Pro]) was purchased from AnaSpec (Fremont, CA, USA). We purchased 2′,7′-dichlorodihydrofluorescein diacetate (DCFH-DA) from Sigma-Aldrich (St. Louis, MO, USA).

Preparation of mini-module dialyzer

We prepared a mini-module dialyzer (miniMD) containing 50 hollow fiber membranes (Supporting Information Figure S2A). The 50 fibers obtained from the dialyzers were placed in an open-ended polycarbonate housing 12-cm long and 5.0 mm in inner diameter. Next, both ends of the bundle were potted with liquid urethane and cured to make solid urethane. The excess solid urethane ends

were then cut to make flat surfaces and open the hollow fiber ends. Finally, inlet and outlet ports were attached to the housing. The assembled miniMD had two compartments; the blood-side compartment (inside the hollow fibers) and dialysate-side compartment (outside the hollow fibers).

Preparation of whole blood, platelets, and neutrophils

Venous whole blood, anticoagulated with acid citrate dextrose solution (3.8 mM citric acid, 7.5 mM trisodium citrate, 13.6 mM dextrose) or heparin (50 U/mL) was obtained from healthy blood donors and used for whole blood experiments or the preparation of cells within 30 min from blood collection. Data obtained with whole blood/cells from one blood donor were considered as one experiment. Heparinized human blood used for the preparation of neutrophils was mixed with an equal volume of 2% dextran in saline, and most of the erythrocytes were allowed to sediment out for 40 min. The leukocyte-rich supernatant was then subjected to Ficoll-Paque PLUS (GE Healthcare UK Ltd., Little Chalfont, Buckinghamshire, UK) density gradient centrifugation at $1300 \times g$ for 20 min. Residual erythrocytes were removed by hypotonic lysis (BD Biosciences, Franklin Lakes, NJ, USA) with a resulting purity of >95% neutrophils as assessed by flow cytometric analysis of the expression of CD33 and CD11b.

Adhesion of platelets to the inner surface of dialysis membrane

The HD membrane was cut lengthwise in half to expose its inner surface, placed on the plastic sheet (Supporting Information Figure S3), and incubated with whole blood for 1 h at 37°C with continuous agitation. In the study of the molecular mechanisms, blood was pretreated with 2 mM Cyclo-GRGDSP, 10 μg/mL anti-GPIIb/IIIa antibody, 10 μg/mL anti-GPIa antibody, or 10 μg/mL anti-GPIb antibody for 10 min at 37°C and thereafter the blood was exposed to the inner surface of the membranes in the presence of the antagonists. After incubation, the membranes were rinsed with saline three times to remove nonadherent cells. The membranes were then fixed in 2.5% glutaraldehyde in saline for 1 h, rinsed several times with distilled water, and dehydrated in a graded ethanol series. The samples were critical point dried and platinum sputtered. Then the specimens were examined with a Field Emission Scanning Electron Microscope (SEM) (S-800 or S-4800, Hitachi High-Technologies Corp., Tokyo, Japan) at an

accelerating voltage of 3 to 5 kV. The adherent platelets on the inner surface of HD membranes in the SEM pictures of 20 random fields (enlargement ×1500, area 4.3×10^3 μm^2) were counted manually for each specimen. When more than 100 adherent platelets were observed in one field, the count of adherent platelets was censored at 100. For evaluation of morphological change in the adherent platelets on HD membranes, photographs of 9 to 10 random fields (enlargement ×5000, area 6.1×10^2 μm^2) for CX-U, APS-SA, PES-SEαeco and Fx-CorDiax were taken. Because only a small number of platelets were observed on NV-U, photographs of five fields including adherent platelets for NV-U were taken. The shape of adherent platelets in the photographs was categorized into five morphological forms defined as follows (18): round or discoid (Round), dendritic (Dendritic) or early pseudopodial, spread dendritic (Spread dendritic) or intermediate pseudopodial, spreading (Spreading), and fully spread (Fully spread).

Treatment of platelets and neutrophils with small pieces of HD membrane

The HD membranes were cut into small pieces 1–2 mm in length, rinsed with sterile saline, and stored in sterile saline until use. The small pieces of membrane (derived from 100-cm length of hollow fibers) were added to 2×10^6 neutrophils suspended in 200 μL of human plasma and incubated at 37°C for 30 min followed by flow cytometric analysis of intracellular production of reactive oxygen species (ROS) and cell-surface activated CD11b, as described later. In the study of the molecular mechanisms, neutrophils were pretreated with 5 mM Cyclo-GRGDSP, 20 μg/mL anti-CD11b antibody, 20 μg/mL anti-αvβ3 antibody, combination of 20 μg/mL anti-CD11b antibody and 20 μg/mL anti-αvβ3 antibody, or 40 μg/mL isotype control IgG (mouse IgG1κ) for 10 min at 37°C before adding small pieces of membrane.

Hemoperfusion of mini-MD in vitro

Supporting Information Figure S2B shows the in vitro hemoperfusion model system. The blood-side compartment of the miniMD was connected to a peristaltic pump through silicon tube lines (Tigers Polymer, Osaka, Japan, 120-cm long with inner diameter 1 mm and outer diameter 3 mm) and the dialysate side compartment of the miniMD was closed to avoid any ultrafiltration. Distilled water was circulated to the blood side at 1 mL/min for more than 5 min, followed by the circulation of phosphate buffered saline (PBS) for 30 min to clean it. Subsequently, whole blood (5 mL) was circulated at a flow rate of 1 mL/min through the circuit at 37°C, and blood samples were collected to analyze activation of neutrophils and granulocytes, or to measure adsorbed fibrinogen. A similar silicone-tube circuit without the miniMD was used for sham perfusion.

Flow cytometric analysis of intracellular production of ROS and cell-surface activated CD11b

Whole blood was circulated through the miniMD containing HD membranes for 10 min, as described above. The blood was stained with PE-conjugated, anti-activated CD11b antibody and FITC-conjugated anti-CD33 antibody for the analysis of cell surface expression of activated CD11b on neutrophils. For analysis of ROS production in granulocytes, the blood was stained with DCFH-DA (0.1 mM at a final concentration) for 15 min at room temperature. The blood was then fixed and lysed by addition of FACS lysing solution (BD Bioscience). After several washes, the cells were suspended in PBS containing 2% fetal calf serum and 0.02% NaN$_3$, and subjected to flow cytometry analysis.

Isolated neutrophils treated with small pieces of HD membrane in plasma were stained with PE-conjugated anti-activated CD11b antibody and DCFH-DA (0.1 mM at a final concentration) at 37°C for 15 min. The neutrophils were fixed with 1 mL of 1% paraformaldehyde in PBS at room temperature for 20 min. After washing and resuspension in modified Tyrode's buffer (137 mM NaCl, 2.8 mM KCl, 1 mM MgCl$_2$, 12 mM NaHCO$_3$, 0.4 mM Na$_2$HPO$_4$, 0.35% BSA, 10 mM Hepes, 5.5 mM D-glucose, pH 7.4), the fixed neutrophils were subjected to flow cytometry analysis.

The fluorescence intensity of the cells (5000 events) was analyzed using a Gallios flow cytometer (Beckman Coulter) and data was analyzed using FlowJo version X software (FlowJo LLC, Ashland, OR, USA). Neutrophils in whole blood were identified as CD33 low-positive cells in a CD33-FITC and side-scatter dot plot. Granulocytes in whole blood and isolated neutrophils were gated according to their size and granularity on a forward-scatter versus side-scatter dot plot. The ROS production was detected by measuring the intracellular oxidized form of DCFH on flow cytometric analysis. Results of activated CD11b expression were expressed as the mean fluorescence intensity, which was calculated as the mean fluorescence intensity of cells stained by each specific antibody subjected

by the mean fluorescence intensity of cells by respective isotype-matched control antibody. Results of ROS production were expressed as the mean fluorescence intensity, which was calculated as the mean fluorescence intensity of cells stained by DCFH-DA subjected by the mean fluorescence intensity of unstained cells.

### Adsorption of fibrinogen onto the HD membrane

HD membranes were obtained from the miniMD after the hemoperfusion for 1 h described above. The membranes (derived from 24-cm long hollow fibers) were cut into pieces about 1 mm in length, and washed with PBS more than three times, followed by three washes with PBS containing 0.1% skim milk and 0.05% Tween. Horseradish peroxidase-conjugated anti-fibrinogen polyclonal antibody (Abcam, Cambridge, UK) was added to the membrane and incubated for 2 h at room temperature. After four washes with PBS containing 0.1% skim milk and 0.05% Tween, the membranes were incubated with 3,3′,5,5′-tetramethylbenzidine (TMB) solution (Promega, Madison, WI, USA) and the absorbance at 450 nm was then determined as an index of the adsorption of fibrinogen, using a microtiter plate reader (TOSOH, Tokyo, Japan). Relative adsorption of fibrinogen onto each HD membrane (%) was calculated by defining the adsorption of fibrinogen onto NV-U as 100%.

Statistical analysis

Data were presented as the mean ± standard error of the mean (SEM). Statistical significance was determined using the SAS System (SAS Institute, Cary, NC, USA). Statistical analysis was performed using an F test followed by a t-test or Welch's test for two groups, or using Bartlett's test followed by Dunnett's, nonparametric Dunnett's, or nonparametric Tukey's multiple comparison for more than three groups. Differences were considered significant when the P value was <0.05.

Ethics statement

This study was reviewed by the Human Tissue Samples Ethics Committee for R&D Toray Industries, Inc. and approved by the chairperson of said committee in compliance with the Human Tissue Samples Ethics Rules for R&D Toray Industries, Inc. All blood donors were informed about the study procedure and provided informed consent.
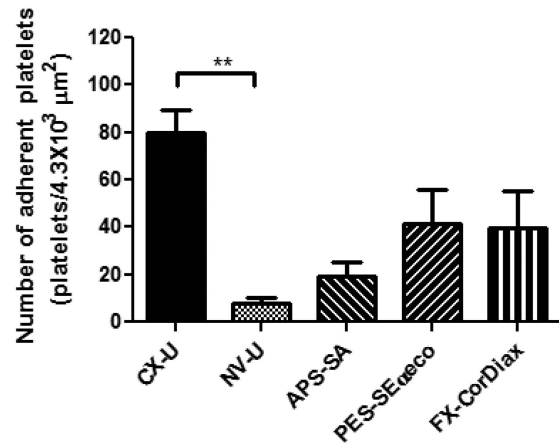
FIG. 1. Number of platelets adherent to the inner surface of hemodialysis (HD) membranes. Data are presented as mean ± SEM of eight independent experiments (using eight different blood donors, respectively). **: $P < 0.01$ between CX-U and NV-U (nonparametric Tukey's multiple comparison).

RESULTS

Number and morphological change of adherent platelets

The degree of platelet activation induced by various HD membranes was evaluated in vitro by analyzing the number and the morphological changes of adherent platelets on the HD membranes, with the use of whole blood.

Figure 1 shows the number of adherent platelets on the inner surface of HD membranes. The greatest number of platelets adhered to CX-U, and many platelets also adhered to PES-Seαeco and FX-CorDiax membranes, respectively. In contrast, the number of adherent platelets was least with NV-U and relatively few platelets adhered to APS-SA.

Morphological changes in platelets adhering to membranes were assessed by categorizing their shape into five morphological forms that describe the extent of platelet spreading (18) (Fig. 2). As a result, platelets on CX-U, PES-Seαeco and FX-CorDiax were mostly fully spread, spreading, or spread dendritic forms. NV-U induced minimal shape changes with mainly a round form and a few fully spread, spreading, or having spread dendritic forms. Platelets on APS-SA were spread to a greater extent than those on NV-U, with most adopting a spread dendritic shape.

These results show that the activation of adherent platelets was very different depending on the membranes used. Among the five tested HD membranes, NV-U and CX-U induced the lowest and highest activation of platelets, respectively.
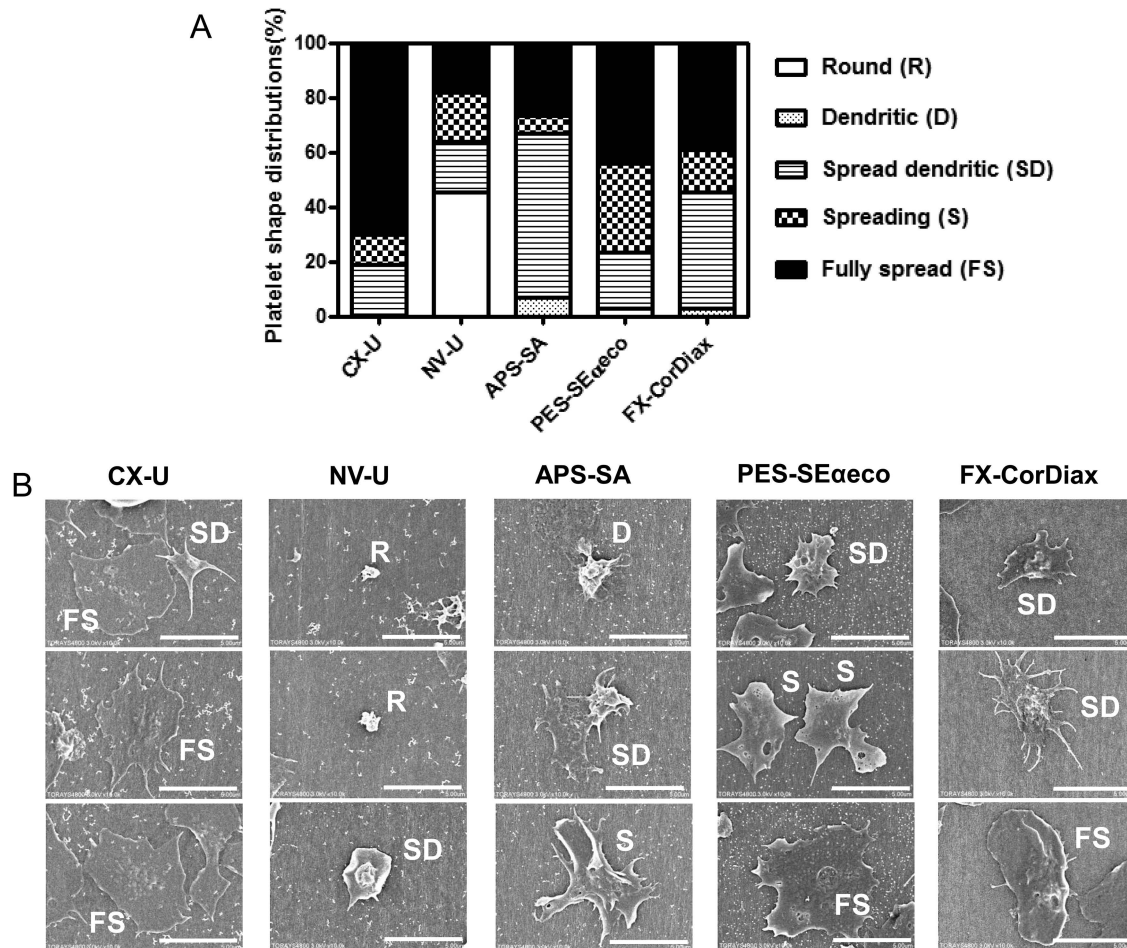
FIG. 2. Morphological changes in platelets adherent to hemodialysis (HD) membranes. (A) Platelet shape distributions for different HD membranes. The shape of adherent platelets in the SEM pictures of 5 to 20 fields (enlargement × 5000, area 6.1×10^2 μm^2) for each HD membrane was categorized. Each histogram shows the relative percentage of platelets in each of five morphological forms: round or discoid (R), dendritic (D) or early pseudopodial, spread dendritic (SD) or intermediate pseudopodial, spreading (S), and fully spread (FS). (B) Representative scanning electron micrographs of human platelets adherent to different HD membranes are shown (scale bar = 5 μm, enlargement ×10 000).

Involvement of integrin receptors in platelets adhesion

We assessed the effects of platelet adhesion receptors antagonists on platelet adhesion to elucidate the molecules involved in the interaction between platelets and membranes. In this study, CX-U and NV-U were used as representative membranes because CX-U induced the greatest platelet adhesion among the five test membranes, while NV-U showed least platelet adhesion. We found that adhesion of platelets to CX-U was almost completely inhibited by an Arg-Gly-Asp (RGD)-dependent integrin antagonist, GRGDSP peptide or anti-integrin glycoprotein (GP) IIb/IIIa (GPIIb/IIIa) antibody, and inhibited to a very slight extent by anti-integrin GPIa antibody or anti-integrin

GPIb antibody (Fig. 3A,B). Similarly, adhesion of a small number of platelets to NV-U was suppressed by GRGDSP peptide or anti-GPIIb/IIIa antibody (Fig. 3C,D). These results suggested that integrin GPIIb/IIIa-mediated interaction with CX-U or NV-U plays a major role in platelet activation.

Activated CD11b expression and ROS production by neutrophils

In vitro biocompatibility of biomaterials is usually evaluated by determining platelet adhesion and the amount of adsorbed protein (13); however, leukocyte activation is also an essential issue in HD therapy. Among leukocytes, we focused on granulocytes, particularly neutrophils that are by far the most prevalent type of granulocytes in the present
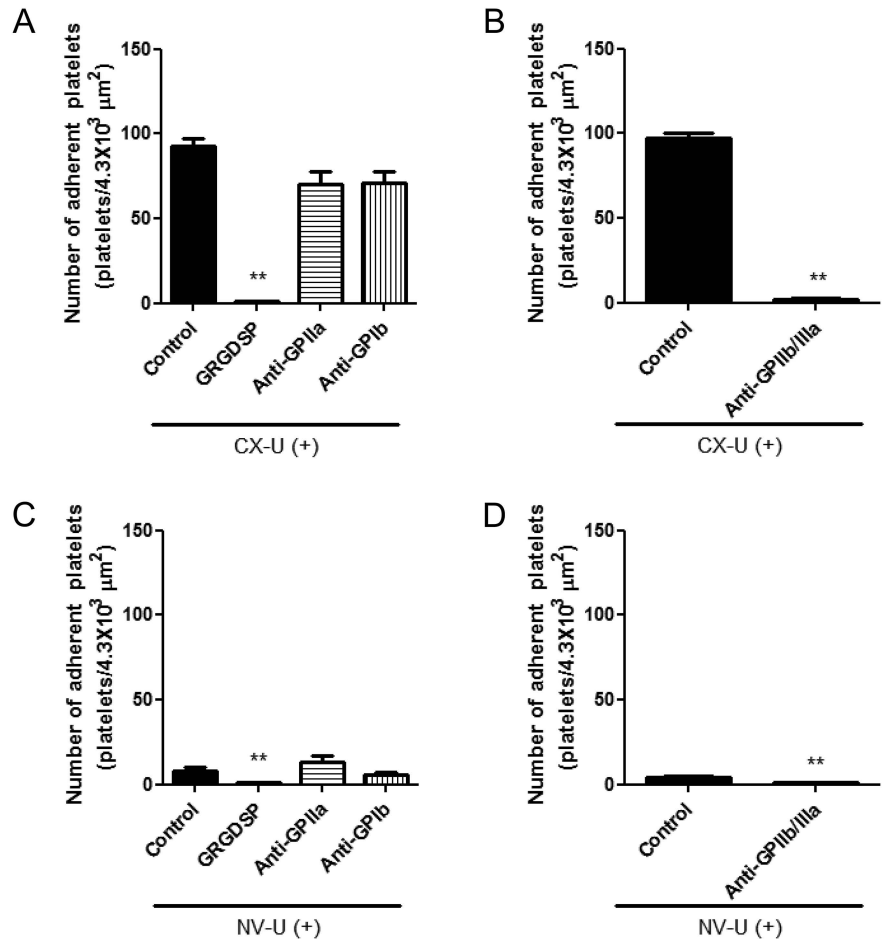
FIG. 3. Effects of integrin antagonists on adhesion of platelets to hemodialysis (HD) membranes. Data are presented as mean ± SEM of 20 SEM fields obtained from duplicate specimens from one representative experiment. The HD membranes used were CX-U (A and B) and NV-U (C and D). **: $P<0.01$ versus Control (nonparametric Dunnett's multiple comparison or Welch's test).

study because an activated neutrophil is an important source of ROS. We then measured cell surface expression of activated CD11b and ROS production of granulocytes or neutrophils as indexes of the degree of neutrophil activation induced by CX-U and NV-U.

Initially, we did not use isolated neutrophils, instead using a whole blood sample to study neutrophils under physiological conditions. CX-U induced an increase in cell-surface expression of activated CD11b on neutrophils and ROS production by granulocytes in whole blood (Fig. 4C,F). Conversely, NV-U caused only slight or almost no increase in cell surface activated CD11b and slight production of ROS (Fig. 4C,F). These results suggested that activation of neutrophils was significantly different between CX-U and NV-U.

Next, we proceeded to investigate mechanisms of neutrophil activation using purified neutrophils, because whole blood is too complicated a system in which to conduct further studies. Previous studies (19–21) reported that HD membranes stimulated

neutrophils indirectly via CD62P-mediated platelet stimulation, while we studied whether HD membranes stimulate neutrophils directly or not—showing that CX-U increased surface expression of activated CD11b and ROS production of neutrophils in the absence of other blood cells (Fig. 5C,D). In contrast to CX-U, neutrophils treated with NV-U showed virtually no or just a slight increase in the expression of activated CD11b and the production of ROS (Fig. 5C,D). These results suggested that CX-U could stimulate neutrophils directly; however, NV-U caused minimal stimulation. This finding is the report of direct stimulation of neutrophils by HD membranes and complements previous studies (19–21).

In summary, CX-U significantly activated neutrophils, while NV-U hardly activated neutrophils. In addition, neutrophils can be activated by a HD membrane through at least two interactions; CD62P-mediated interaction with platelets activated by the HD membrane (19–21) as well as direct interaction with the HD membrane.
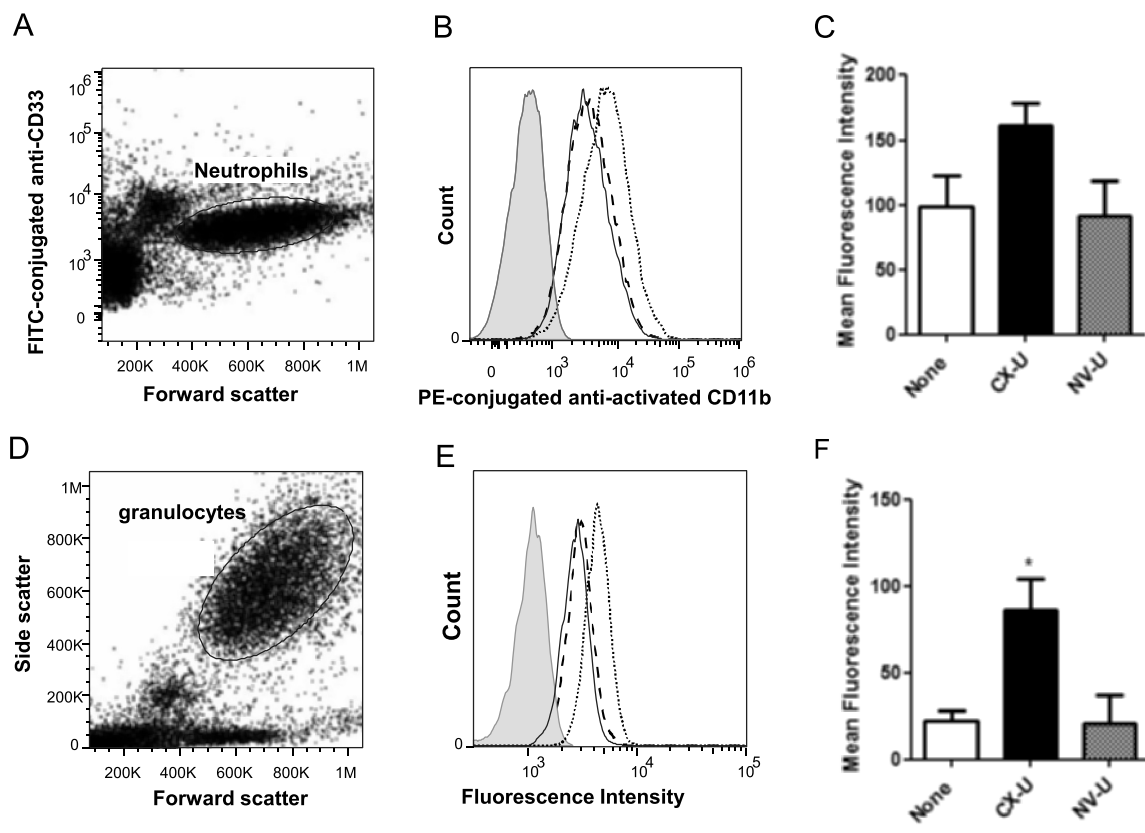
FIG. 4. Activation of neutrophils induced by hemodialysis (HD) membranes in whole blood. The fluorescence intensity of cells was analyzed by flow cytometry. Neutrophils were identified as CD33 low-positive cells in forward scatter versus log fluorescence of FITC-conjugated anti-CD33 dot plot (A). (B) A representative flow cytometry histogram plot showing expression of activated CD11b on neutrophils. Filled histogram, cells with isotype control; solid line, cells without miniMD (None group); dotted line, cells of CX-U miniMD; dashed line, cells of NV-U miniMD. (C) Expression of activated CD11b on neutrophils. (D) Granulocytes were gated in forward scatter versus side scatter dot plot. (E) A representative flow cytometry histogram plot showing production of ROS. Filled histogram, autofluorescence of cells; solid line, cells without miniMD (None group); dotted line, cells of CX-U miniMD; dashed line, cells of NV-U miniMD. (F) Production of ROS on neutrophils. The ROS production in neutrophils was detected by measuring the intracellular oxidized form of DCFH. Each column represents as mean $\pm$ SEM of three independent experiments (using three different blood donors, respectively) *: $P < 0.05$ versus None (Dunnett's multiple comparison).

**Involvement of integrin receptors in neutrophil ROS production**

We investigated the molecular mechanisms of neutrophil ROS production directly induced by CX-U and NV-U. The production of ROS in neutrophils directly induced by CX-U was greatly inhibited by GRGDSP peptide. Anti-CD11b (integrin α subunit of Mac-1) antibody or anti-integrin $\alpha v\beta3$ ($\alpha v\beta3$) antibody alone partially inhibited ROS production in neutrophils by CX-U; however, combining the antibodies causes additive inhibition (Fig. 6A). Similarly, the small amount of production of ROS in neutrophils induced by NV-U was inhibited by GRGDSP peptide or the combination of antibodies (Fig. 6B). These results suggested that the Mac-1 and $\alpha v\beta3$-mediated interaction with CX-U or NV-U plays a major role in neutrophil activation.
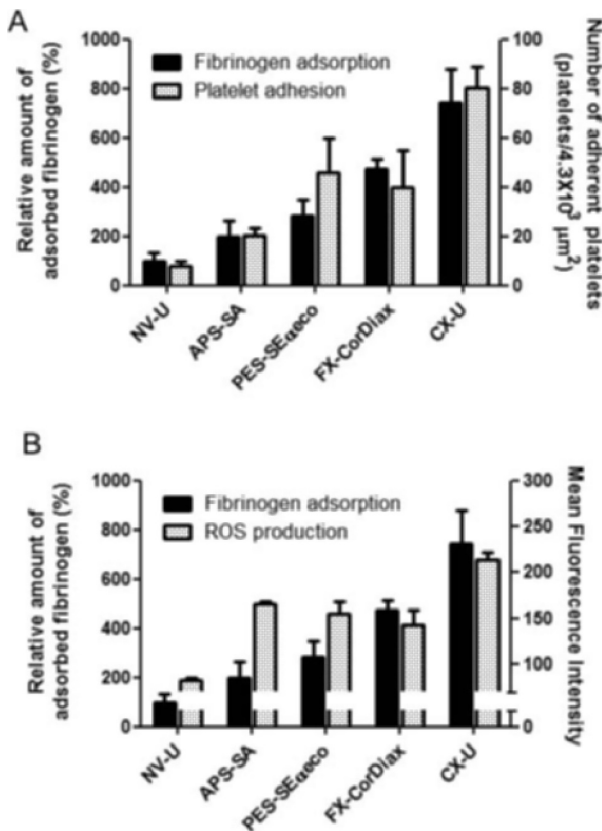
Adsorption of fibrinogen onto membranes

The above studies using antagonists have showed that GPIIb/IIIa, Mac-1, and $\alpha v\beta3$ are functionally essential in the interaction of blood cells with CX-U or NV-U; we next measured the amount of their common ligand, plasma-derived fibrinogen containing an RGD sequence, adsorbed onto HD membranes (Fig. 7). The amount of fibrinogen adsorbed on CX-U was greater than with any other membrane, whereas minimal adsorption of fibrinogen appeared on NV-U. Comparing the amount of adsorbed fibrinogen and the number of adherent platelets among the five PSf membranes, the number of adherent platelets increased with the amount of adsorbed fibrinogen (Fig. 7A). ROS production by neutrophils also tended to increase, depending on the amount of adsorbed fibrinogen (Fig. 7B). In APS-SA alone, ROS production was relatively

A

B

FIG. 5. Activation of purified neutrophils induced by hemodialysis (HD) membranes. The fluorescence of the neutrophils was measured by flow cytometry. (A) Neutrophils were gated in forward scatter versus side scatter dot plot. (B) The isolated cells were CD33 low positive and CD11b high positive in log fluorescence of FITC-CD33 versus log fluorescence of PE-conjugated anti-CD11b dot plot. The expression of activated CD11b (C) and the intracellular oxidized form of DCFH, an index of ROS production (D) are shown. Data are presented as mean ± SEM of three independent experiments (using three different blood donors, respectively). *: $P < 0.05$, **: $P < 0.01$ versus None (Dunnett's or nonparametric Dunnett's multiple comparison).

C

D

A

B
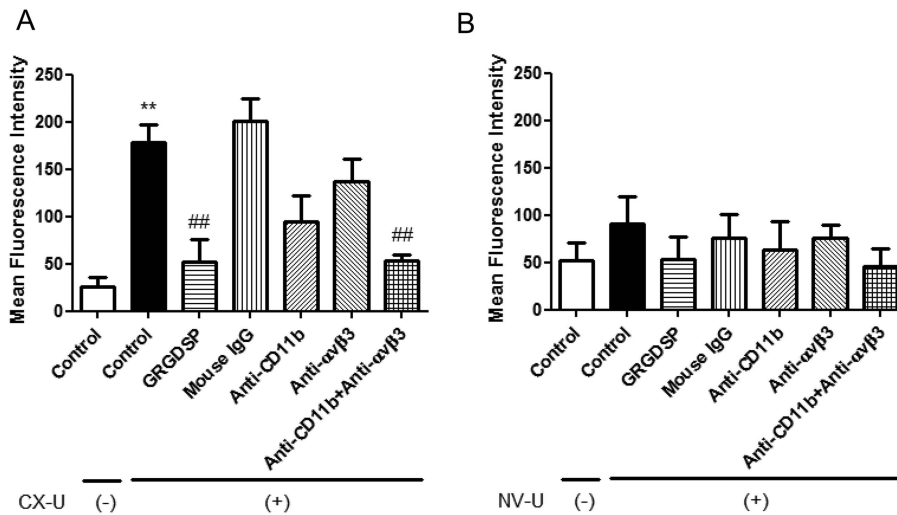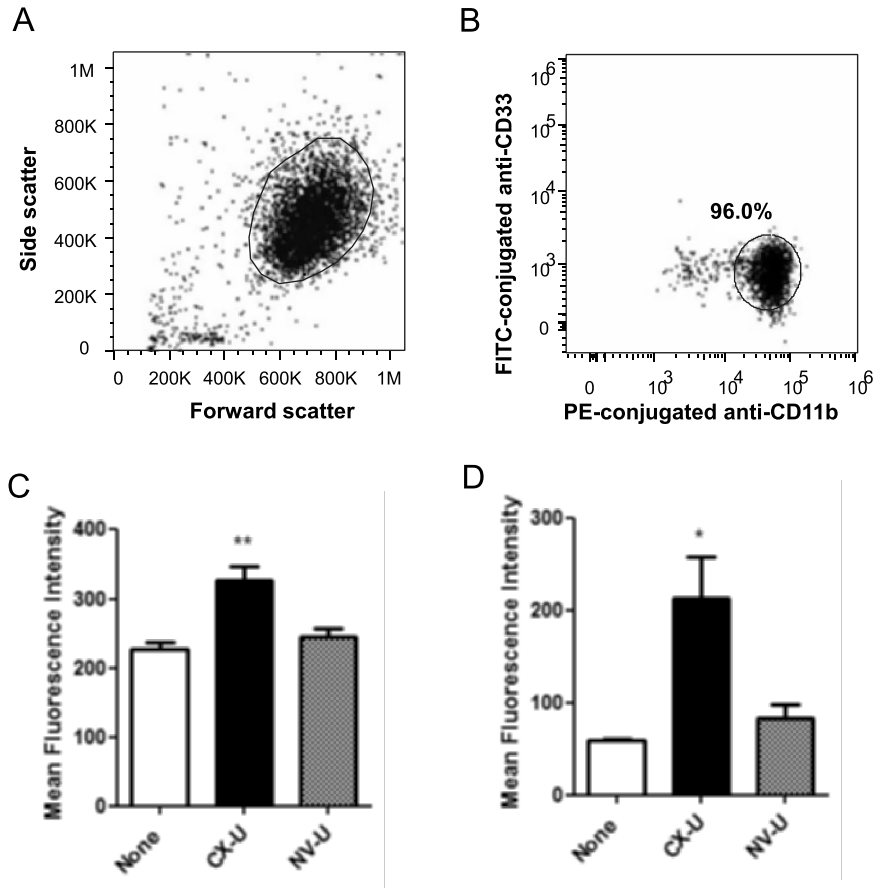
FIG. 6. Effects of integrin antagonists on neutrophil activation induced by CX-U and NV-U. Isolated neutrophils suspended in plasma were treated with small pieces of hemodialysis (HD) membrane or without HD membrane (None group) in the absence or presence of indicated antagonists for 30 min at 37°C, and then stained with DCFH-DA at 37°C for 15 min. The HD membranes used were CX-U (A) and NV-U (B). The fluorescence of the neutrophils was measured by flow cytometry to detect the intracellular oxidized form of DCFH, an index of ROS production. Data are presented as mean ± SEM of triplicate measurements from one representative experiment. **: $P < 0.01$ between Control/CX-U(-) versus Control/CX-U(+) (t-test), ##: $P < 0.01$ versus Control/CX-U(+) (Dunnett's multiple comparison).

FIG. 7. Adsorption of fibrinogen onto hemodialysis (HD) membranes and its relationship to cell responses. The left axis and black columns show the relative adsorption of fibrinogen onto HD membranes. Data shows the relative adsorption of fibrinogen onto each HD membrane (%), defining the adsorption of fibrinogen onto NV-U as 100%. (A) The right axis and dotted columns show the number of platelets adherent to each HD membrane described in Fig. 1. (B) The right axis and dotted columns show the mean fluorescence intensity, which indicates ROS production of neutrophils determined. The fluorescence of the neutrophils was measured by flow cytometry to detect the intracellular oxidized form of DCFH, an index of ROS production. Data for fibrinogen adsorption and ROS production are presented as mean ± SEM of three independent experiments.

high although adsorption of fibrinogen was not high; therefore, it seemed that other factors as well as fibrinogen contributed ROS production on APS-SA.

From these results, the adsorption of fibrinogen on the membrane was closely associated with activation of platelets and neutrophils.

DISCUSSION

In this study, we examined the effect of five commercially available PSf membranes on platelets in vitro and found that these membranes caused different platelet activation, as assessed by the number of and morphological changes in adherent platelets. Specifically, NV-U and CX-U respectively induced the lowest and highest activation of platelets among the tested membranes. This result is probably relevant to observations from a clinical study in which dialysis using NV-U showed smaller changes in platelet parameters than dialysis using CX-U (15).

In our analysis of the molecular mechanisms, we examined the involvement of major platelet integrin receptors, GPIb, GPIa, and GPIIb/IIIa in platelet activation, as assessed by adhesion (22,23). GPIb is part of the GPIb-V-IX complex that functions as a receptor for von Willebrand factor (vWF) and the binding of the GP Ib-IX-V complex to vWF promotes initial platelet adhesion at sites of vascular injury. GPIa is an integrin α2 subunit and associates with GPIIa to form GPIa/IIa (also called integrin α2β1), which is very important for platelet adhesion to collagen. GPIIb/IIIa is an integrin receptor that recognizes the RGD sequence of fibrinogen and plays a major role in platelet aggregation. At a site of vascular injury, all are essential and critically required for establishment of hemostasis, while only GPIIb/IIIa was important in platelet activation by CX-U and NV-U. These results indicate that the cell-surface receptors activating platelets are the same for CX-U and NV-U despite large differences in platelet activation. Consequently, we believe that the type of receptor on platelets does not determine the degree of platelet activation, but that the state of membrane ligands is important, as discussed later.

In addition to platelet activation, we report that activation of neutrophils was substantially different among different PSf membranes. In particular, neutrophils were activated to a greater degree by CX-U than by any other membrane, with minimal activation by NV-U. On analysis of the mechanisms of neutrophil activation, we investigated whether HD membranes stimulate neutrophils directly or not. Regarding this point, previous studies have already showed that HD membranes indirectly stimulated neutrophils by inducing the activation of platelets and subsequent CD62P-mediated adhesion of the activated platelets to neutrophils (19–21). In this study, we found that HD membranes can stimulate neutrophils through a direct interaction with the membranes. This finding complements the previous study of HD-membrane induced neutrophil activation. Taken together, it is apparent that HD membranes can activate neutrophils by both direct and indirect interaction with the membranes. We then investigated the molecular mechanisms of this direct activation of neutrophils by CX-U and NV-

U, examining involvement of the major neutrophil integrin receptors, Mac-1 and αvβ3. Mac-1, also known as the CD11b/CD18 complex, is composed of an integrin αM subunit CD11b and an integrin β2 subunit CD18. Mac-1 is the predominant integrin adhesion molecule mediating neutrophil migration, and several ligands have been described for Mac-1, including ICAM-1 and iC3 as well as fibrinogen (24). The αvβ3 integrin is a receptor for vitronectin and fibrinogen. It is well-known that it is overexpressed in malignant tumors and endothelial cells during neovascularization and plays important roles in malignant growth and angiogenesis. The αvβ3 is also found on neutrophils and mediates the adhesion of neutrophils to the extracellular matrix (25). Our studies using integrin antagonists in Fig. 6 suggested that the activation of neutrophils induced by CX-U or NV-U is mediated by interaction between Mac-1/αvβ3 on neutrophils and their ligand that contains the RGD sequence. Additionally, these results indicate that the cell-surface receptors that activated neutrophils were the same for CX-U and NV-U, despite large differences in neutrophil activation. We thus believe that the type of receptor on neutrophils does not determine the degree of neutrophil activation, but that the state of ligands on the membrane (described later) is considered to be important.

As mentioned above, we used antagonists to directly demonstrate that integrin receptors, GPIIb/IIIa, Mac-1 and αvβ3 are functionally important in the interaction of platelets and neutrophils with CX-U or NV-U, and that these interactions depend on the RGD sequence. In addition, previous studies have described the relationship of fibrinogen deposition and cell adhesion on biomaterials (26,27). Based on these results, we focused on fibrinogen, which is a major ligand of GPIIb/IIIa, Mac-1 and αvβ3 that contains the RGD sequence. We confirmed that the amount of fibrinogen adsorbed on PSf HD membranes was closely related to the number of adherent platelets and ROS production by neutrophils. Regarding APS-SA, ROS production was relatively high although adsorption of fibrinogen was not high; therefore, other ligands, such as complement proteins which could activate neutrophils through Mac-1 and LFA-1-mediated interaction, might contribute ROS production. Summarizing the above, we conclude that fibrinogen adsorbed to PSf HD membranes causes GPIIb/IIIa-mediated platelet activation, and Mac-1/αvβ3-mediated neutrophil activation, depending on the amount of adsorption (Fig. 8). In addition, the amount of fibrinogen adsorbed to the membranes is considered to be the main determinant of the degree of cell activation.

It is known that the hydrophilicity of the membrane surface affects the adsorption of blood components, such as plasma-derived proteins and blood cells, and many PSf based-membranes are combined with a hydrophilic polymer, polyvinylpyrrolidone (PVP) to avoid the adsorption of blood components. However, the efficiency of PVP in preventing protein adsorption onto PSf membrane surfaces was reported to differ, depending on the state of PVP on the inner surface of membranes—factors such as the amount of PVP, its molecular weight, and the degree of cross-linking between PSf and PVP (28,29). We thus speculate that the different states of hydrophilic polymers such as PVP affected adsorption of fibrinogen to the five PSf membranes. Our data in Table 1 on the thickness of the swollen layer of the membrane surface also supported a close association between fibrinogen adsorption and the state of hydrophilic polymers. The thickness of the swollen layer mainly reflects the thickness of the hydrophilic polymer layer on the surface, because hydrophilic polymers swell markedly in wet conditions. Table 1 indicates that NV-U, with its low adsorption of fibrinogen, had the thickest swollen layer; however, CX-U, which has high adsorption of fibrinogen, had the thinnest swollen layer. We therefore believe that there was an inverse relationship between fibrinogen adsorption and the thickness of the swollen layer at the membrane surface. Because NV-U is immobilized with a hydrophilic polymer which is different from PVP (28), this immobilized hydrophilic polymer is considered to contribute to the thickest swollen layer.

There is no difference in surface element compositions among CX-U, NV-U, APS-SA, and FX-CorDiax (Table 2). Compared to these PSf membranes, PES-SECαeco was observed to have a different elemental composition, which can be attributed to the different structure of its material (Table 1).

Considering this information together, different states of hydrophilic polymers on the membrane surface, including their different thickness may result in a different hydrophilic/hydrophobic nature of the membrane surfaces, and subsequent different adsorption of fibrinogen (Fig. 8).

The main limitation of our study is that this is only an in vitro study. Cell activation during hemodialysis plays an important role in microvascular inflammation and oxidative stress in HD patients; however, the causes of inflammatory syndromes
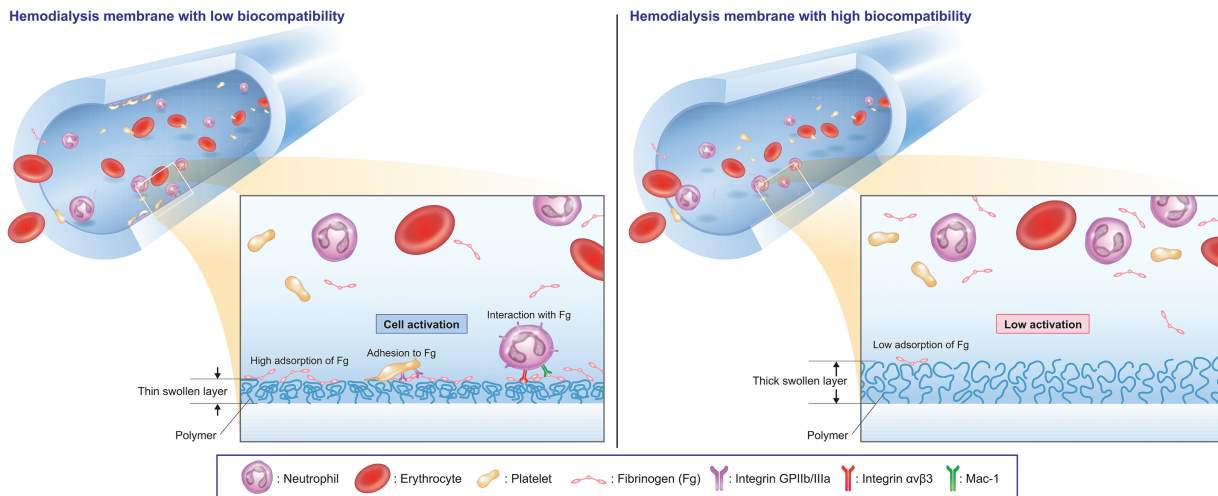
FIG. 8. Schematic illustration showing the means by which hemodialysis membranes affect platelet and neutrophil activation.

in HD patients are multifactorial and include membrane biocompatibility, dialysate quality and patient-related factors, such as underlying diseases. Therefore, we lack sufficient data to support a discussion on the clinical implications of cell activation and more detailed observations in HD patients would be necessary to develop this argument.

Consequently, the use of a biocompatible membrane that is not associated with cell activation, such as NV-U, is expected to reduce microvascular inflammation and oxidative stress in HD patients. Furthermore, these favorable effects may have some benefits in hemodialysis treatment, for example a reduction in various HD-associated complications.

CONCLUSIONS

This study assessed the effects of five polysulfone hemodialysis membranes on blood cells in vitro, and showed that the number of platelets adherent to their surfaces, and ROS production by neutrophils were clearly different among membranes. For example, CX-U induced adhesion of many platelets and increased the surface expression of activated CD11b and ROS production of neutrophils; however, NV-U had virtually no effect on platelets and neutrophils. Study of the molecular mechanisms of these cell

activations demonstrated that adhesion of platelet and ROS production by neutrophils were mediated by GPIIb/IIIa on platelets, and Mac-1 and $\alpha v\beta 3$ on neutrophils, respectively. In addition, the number of adherent platelets and neutrophil ROS production rose with the amount of fibrinogen adsorbed on the membranes. These results suggested that fibrinogen adsorbed on PSf membranes induced GPIIb/IIIa-mediated platelet activation and Mac-1 and $\alpha v\beta 3$-mediated neutrophil activation, depending on the amount of adsorption. In conclusion, we believe that a membrane with lower fibrinogen adsorption may reduce cell activation during dialysis, and subsequent microvascular inflammation and oxidative stress during HD treatment. Furthermore, these favorable effects are expected to decrease the risk of development and progression of various HD-associated complications.

Author Contributions: Yoko Koga: concept/design of the experiment, performed the experiment, data analysis/interpretation, wrote the paper. Hiroaki Fujieda: concept/design of the experiment, performed the experiment, data analysis/interpretation, wrote the paper. Hiroyuki Meguro: concept/design of the experiment, performed the experiment, data analysis/interpretation. Yoshiyuki Ueno: concept/design of the experiment, data analysis/interpretation. Mie Kainoh: concept/design of the experiment, data analysis/interpretation, wrote the paper. Takao Aoki and Keishi Miwa: data analysis/interpretation.

TABLE 2. *Element composition on the inner surface of HD membranes*

Membranes	C (%)	N (%)	O (%)	S (%)
CX-U	81.9	3.3	12.1	2.7
NV-U	81.1	3.2	13.2	2.5
APS-SA	82.1	3.9	11.6	2.3
PES-SEαeco	75.2	3.8	16.1	4.9
FX-CorDiax	82.4	3.0	11.9	2.7

Conflict of Interest: All authors are employees of Toray Industries, Inc.

REFERENCES

1. Daugirdas JT, Bernardo AA. Hemodialysis effect on platelet count and function and hemodialysis-associated thrombocytopenia. *Kidney Int* 2012;82:147–57.
2. Sirolli V, Ballone E, Di Stante S, Amoroso L, Bonomini M. Cell activation and cellular-cellular interactions during hemodialysis: effect of dialyzer membrane. *Int J Artif Organs* 2002;25:529–37.
3. Yoon JW, Pahl MV, Vaziri ND. Spontaneous leukocyte activation and oxygen-free radical generation in end-stage renal disease. *Kidney Int* 2007;71:167–72.
4. Pertosa G, Grandaliano G, Gesualdo L, Schena FP. Clinical relevance of cytokine production in hemodialysis. *Kidney Int Suppl* 2000;58:S104–11.
5. Kakuta T, Komaba H, Takagi N, et al. A prospective multi-center randomized controlled study on interleukin-6 removal and induction by a new hemodialyzer with improved biocompatibility in HD patients: a pilot study. *Ther Apher Dial* 2016;20:569–78.
6. Himmelfarb J, Stenvinkel P, Ikizler TA, Hakim RM. The elephant in uremia: oxidant stress as a unifying concept of cardiovascular disease in uremia. *Kidney Int* 2002;62:1524–38.
7. Kaya Y, Ari E, Demir H, et al. Accelerated atherosclerosis in haemodialysis patients; correlation of endothelial function with oxidative DNA damage. *Nephrol Dial Transplant* 2012;27:1164–9.
8. Hakim RM. Clinical implications of hemodialysis membrane biocompatibility. *Kidney Int* 1993;44:484–94.
9. Ren H, Zhou X, Luan Z, et al. The relationship between carotid atherosclerosis, inflammatory cytokines, and oxidative stress in middle-aged and elderly hemodialysis patients. *Int J Nephrol* 2013;2013:1.
10. Recio-Mayoral A, Banerjee D, Streather C, Kaski JC. Endothelial dysfunction, inflammation and atherosclerosis in chronic kidney disease–a cross-sectional study of predialysis, dialysis and kidney-transplantation patients. *Atherosclerosis* 2011;216:446–51.
11. Khalil SK, Amer HA, El Behairy AM, Warda M. Oxidative stress during erythropoietin hyporesponsiveness anemia at end stage renal disease: molecular and biochemical studies. *J Adv Res* 2016;7:348–58.
12. Cai Q, Mukku VK, Ahmad M. Coronary artery disease in patients with chronic kidney disease: a clinical update. *Curr Cardiol Rev* 2013;9:331–9.
13. Hayama M, Yamamoto K, Kohori F, Sakai K. How polysulfone dialysis membranes containing polyvinylpyrrolidone achieve excellent biocompatibility?. *J Membr Sci* 2004;234:41–9.
14. Hoenich NA, Woffindin C, Brennan A, Cox PJ, Matthews JN, Goldfinch M. A comparison of three brands of polysulfone membranes. *J Am Soc Nephrol* 1996;7:871–6.
15. Yamaka T, Ichikawa K, Saito M, et al. Biocompatibility of the new anticoagulant dialyzer TORAYLIGHT NV. *Sci Postprint* 2014;1:1–5.
16. Hidaka S, Kobayashi S, Maesato K, et al. Hydrophilic polymer-coated polysulfone membrane improves endothelial function of hemodialysis patients: a pilot study. *J Clin Nephrol Res* 2015;2:1020–4.
17. Cappella B, Dietler G. Force-distance curves by atomic-force microscopy. *Surf Sci Rep* 1999;34:1–104.
18. Goodman SL. Sheep, pig, and human platelet-material interactions with model cardiovascular biomaterials. *J Biomed Mater Res* 1999;45:240–50.
19. Itoh S, Takeshita K, Susuki C, Shige-Eda K, Tsuji T. Redistribution of P-selectin ligands on neutrophil cell membranes and the formation of platelet-neutrophil complex induced by hemodialysis membranes. *Biomaterials* 2008;29:3084–90.
20. Itoh S, Susuki C, Tsuji T. Platelet activation through interaction with hemodialysis membranes induces neutrophils to produce reactive oxygen species. *J Biomed Mater Res* 2006;77A:294–303.
21. Bonomini M, Stuard S, Carreno MP, et al. Neutrophil reactive oxygen species production during HD: role of activated platelet adhesion to neutrophils through P-selectin. *Nephron* 1997;75:402–11.
22. Li Z, Delaney MK, O'Brien KA, Du X. Signaling during platelet adhesion and activation. *Arterioscler Thromb Vasc Biol* 2010;30:2341–9.
23. Rivera J, Lozano ML, Navarro-Núñez L, Vicente V. Platelet receptors and signaling in the dynamics of thrombus formation. *Haematologica* 2009;94:700–11.
24. Altieri DC, Agbanyo FR, Plescia J, Ginsberg MH, Edgington TS, Plow EF. A unique recognition site mediates the interaction of fibrinogen with the leukocyte integrin Mac-1 (CD11b/CD18). *J Biol Chem* 1990;265:12119–22.
25. Lindbom L, Werr J. Integrin-dependent neutrophil migration in extravascular tissue. *Semin Immunol* 2002;14:115–21.
26. Sivaraman B, Latour RA. Delineating the roles of the GPIIb/IIIa and GP-Ib-IX-V platelet receptors in mediating platelet adhesion to adsorbed fibrinogen and albumin. *Biomaterials* 2011;32:5365–70.
27. Safiullin R, Christenson W, Owaynat H, et al. Fibrinogen matrix deposited on the surface of biomaterials acts as a natural anti-adhesive coating. *Biomaterials* 2015;67:151–9.
28. Oshihara W, Ueno Y, Fujieda H. A new polysulfone membrane dialyzer, NV, with low-fouling and antithrombotic properties. *Contrib Nephrol* 2017;76:222–9.
29. Hayama M, Yamamoto K, Kohori F, et al. Nanoscopic behavior of polyvinylpyrrolidone particles on polysulfone/polyvinylpyrrolidone film. *Biomaterials* 2004;25:1019–28.

SUPPORTING INFORMATION

Additional supporting information may be found online in the Supporting Information section at the end of the article.

FIG. S1. The force-distance curve measured by atomic-force microscopy. A. Process used to approximate atomic-force microscopy probe to sample. B. Schematic representation of the force–distance curve.

FIG. S2. Schematic representation of mini-module dialyzer (miniMD) (A) and in vitro hemoperfusion model system (B).

FIG. S3. Schematic representation of preparation of HD membranes for platelet adhesion assays. A. Put a plastic sheet (diameter: 18 mm) between double-sided tapes. B. Put the HD membranes on the double-sided tape. C. Place stainless plates (thickness: 0.15 mm) on both sides of the membrane. D. Cut the membranes by sliding a razor along the stainless plates.